

Strangeness $S = -2$ baryon-baryon interaction at next-to-leading order in chiral effective field theory

J. Haidenbauer^{1,2}, Ulf-G. Meißner^{1,2,3}, S. Petschauer⁴

¹*Institute for Advanced Simulation, Forschungszentrum Jülich, D-52425 Jülich, Germany*

²*Institut für Kernphysik (Theorie) and Jülich Center for Hadron Physics, Forschungszentrum Jülich, D-52425 Jülich, Germany*

³*Helmholtz Institut für Strahlen- und Kernphysik and Bethe Center for Theoretical Physics, Universität Bonn, D-53115 Bonn, Germany*

⁴*Physik Department, Technische Universität München, D-85747 Garching, Germany*

The strangeness $S = -2$ baryon-baryon interaction is studied in chiral effective field theory up to next-to-leading order. The potential at this order consists of contributions from one- and two-pseudoscalar-meson exchange diagrams and from four-baryon contact terms without and with two derivatives. $SU(3)$ flavor symmetry is imposed for constructing the interaction in the $S = -2$ sector. Specifically, the couplings of the pseudoscalar mesons to the baryons are fixed by $SU(3)$ symmetry and, in general, also the contact terms are related via $SU(3)$ symmetry to those determined in a previous study of the $S = -1$ hyperon-nucleon interaction. The explicit $SU(3)$ symmetry breaking due to the physical masses of the pseudoscalar mesons (π , K , η) is taken into account. It is argued that the ΞN interaction has to be relatively weak to be in accordance with available experimental constraints. In particular, the published values and upper bounds for the $\Xi^- p$ elastic and inelastic cross sections apparently rule out a somewhat stronger attractive ΞN force and, specifically, disfavor any near-threshold deuteron-like bound states in that system.

PACS numbers: 13.75.-n,13.75.Ev,12.39.Fe,25.80.Pw

I. INTRODUCTION

The interaction between baryons in the strangeness $S = -2$ sector ($\Lambda\Lambda$, ΞN , $\Sigma\Lambda$, $\Sigma\Sigma$) has been in the focus of interest for many years. Here, the so-called H -dibaryon has certainly played a prominent role. The H -dibaryon, a deeply bound 6-quark state with $S = -2$, $J = 0$ and isospin $I = 0$, was predicted by Jaffe within the bag model [1] and should appear in the coupled $\Lambda\Lambda - \Xi N - \Sigma\Sigma$ system. So far none of the experimental searches for the H -dibaryon led to convincing signals [2, 3]. Recently, evidence for a bound H -dibaryon was claimed based on lattice QCD calculations [4–6]. Extrapolations of those computations, performed for $m_\pi \gtrsim 400$ MeV, to the physical pion mass suggest, however, that most likely the H -dibaryon disappears into the continuum [7–12].

The interaction in the strangeness $S = -2$ sector has also gained increasing importance in discussions on the properties of neutron stars in the context of the problem known as the “hyperon puzzle” [13]. It concerns the observation of two-solar-mass neutron stars [14, 15] which provides particularly strong restrictions for the appearance of hyperons in neutron stars. The latter leads to a softening of the equation-of-state (EoS) and to a reduction of the attainable maximum mass. A repulsive hyperon-hyperon (YY) interaction is seen as one of the possible mechanisms that could generate additional repulsion so that the EoS remains sufficiently stiff [16–20], as is required for the explanation of neutron stars with such high masses.

Another debated issue is the existence of Ξ hypernuclei [21–23]. The observed spectrum of the (K^- , K^+) reaction on a ^{12}C target [24] has been viewed as indication for a moderately attractive ΞN interaction. In particular, an initial analysis of this reaction resulted in an attractive Ξ potential of $U_\Xi \approx -14$ MeV [24]. On the other hand, a re-analysis by Kohno et al. came to the conclusion that an almost zero [25] or even a weakly repulsive Ξ potential [26] is preferable. Very recently first evidence for the existence of a deeply bound Ξ^- - ^{14}N system was claimed [27], that again would be indicative for at least some attraction. On the extreme side, there are speculations that the ΞN interaction could be much more strongly attractive [28] so that even ΞNN bound states could exist.

We present an investigation of the baryon-baryon (BB) interaction in the strangeness $S = -2$ sector within SU(3) chiral effective field theory (EFT). The work is an extension of our previous leading-order study [29] to next-to-leading order (NLO) in the chiral expansion. Chiral EFT as a tool to treat the interaction between baryons was initially proposed by Weinberg [30, 31] for the nucleon-nucleon (NN) system and rather successfully put into practice in a series of works by Epelbaum et al. [32, 33] and Entem and Machleidt [34, 35], see also the reviews [36, 37]. The application of this scheme to the hyperon-nucleon (YN) sector [38–40] led to satisfying results as well. Specifically, as demonstrated in Ref. [40], at NLO in chiral EFT the ΛN and ΣN scattering data can be reproduced with the same level of quality as by the most advanced meson-exchange YN interactions. Furthermore, the properties of hyperons in nuclear matter are nicely described with such an NLO interaction [41, 42]. Therefore, it is timely to also provide now a NLO BB interaction for the $S = -2$ sector. Nevertheless, it has to be said that the overall situation is not that encouraging because of the lack of pertinent scattering data for the $\Lambda\Lambda$, $\Sigma\Sigma$ and ΞN systems. Indeed, there are just a few data points and upper bounds for the ΞN elastic and inelastic cross sections [43–45] that put constraints on the corresponding interactions. Clearly, the use of chiral EFT cannot overcome that problem already faced by phenomenological approaches to the BB interaction in the $S = -2$ sector [46–50]. However, once more data will be available, chiral EFT is the premier framework to analyze these.

We begin with providing an overview of the available experimental information and constraints on the $\Lambda\Lambda$ and ΞN interactions (in Sect. II), and then proceed with a brief introduction to the concepts and formalism of chiral EFT. This approach exploits the symmetries of QCD together with the appropriate low-energy degrees of freedom to construct the BB interaction. Essential features of chiral EFT are that the results can be improved systematically by going to higher order in the power counting scheme, and that two- and three-baryon forces can be calculated in a consistent way [51]. At the order we are working the chiral interaction consists of BB contact terms without derivatives and with two derivatives, together with contributions from one-pseudoscalar-meson exchanges and from (irreducible) two-pseudoscalar-meson exchanges [40]. The corresponding diagrams are shown schematically in Fig. 1. The contributions from pseudoscalar-meson exchanges to the BB interaction are completely fixed by the assumed SU(3) flavor symmetry. On the other hand, the strength parameters associated with the contact terms, the low-energy constants (LECs), need to be determined in a fit to data. How this is done is discussed in Sect. III in detail. We impose SU(3) symmetry also for the contact terms which reduces the number of independent LECs that can contribute significantly. Furthermore, in general, we exploit SU(3) symmetry to relate the LECs needed in the $S = -2$ sector to those fixed in our fit to the $S = -1$ YN data before [40].

Results for $\Lambda\Lambda$ and ΞN scattering are presented in Sect. IV. As the main outcome, those indicate that the ΞN interaction has to be relatively weak if one takes the available experimental information and, in particular, the published upper bounds for cross sections into consideration. A weak ΞN interaction has been already predicted by our leading-order (LO) interaction [29] and also by several phenomenological models of the BB interaction in the $S = -2$ sector [47, 49, 52].

The paper closes with a Summary and with an Appendix that contains some technical details.

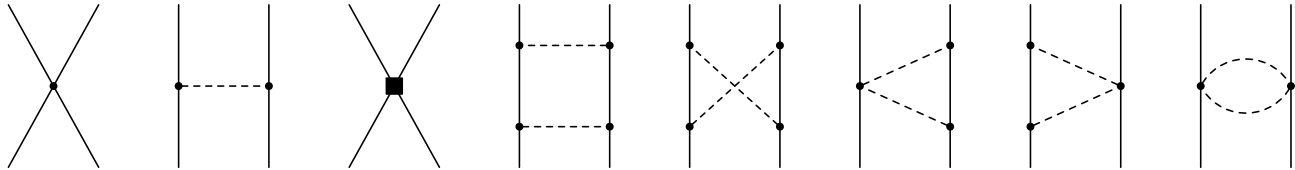


FIG. 1. Relevant Feynman diagrams up-to-and-including next-to-leading order. Solid and dashed lines denote octet baryons and pseudoscalar mesons, respectively. The square symbolizes a contact vertex with two derivatives. From left to right: LO contact term, one-meson exchange, NLO contact term, planar box, crossed box, left triangle, right triangle, football diagram. From the planar box graph, only the irreducible part contributes to the potential.

II. AVAILABLE EXPERIMENTAL INFORMATION

Before we come to our calculation let us briefly review the experimental situation for the strangeness $S = -2$ sector. Unfortunately, there are practically no genuine scattering data for the $\Lambda\Lambda$ and ΞN systems at low energies. However, there is other information from few- and many-baryon systems that allows one to put at least some qualitative constraints on the baryon-baryon interaction with strangeness $S = -2$. Those constraints are used as guideline in the construction of our interaction.

A. The $\Lambda\Lambda$ system

To our knowledge there are no scattering data for $\Lambda\Lambda$. However, available experimental information on double- Λ hypernuclei put fairly tight constraints on the $\Lambda\Lambda$ 1S_0 scattering length. Specifically, the unambiguously identified ${}_{\Lambda\Lambda}^6\text{He}$ hypernucleus (Nagara event) [53] plays an important role in this context. The analysis of that event yielded the fairly small separation energy of $\Delta B_{\Lambda\Lambda} = B_{\Lambda\Lambda}({}_{\Lambda\Lambda}^6\text{He}) - 2B_{\Lambda}({}_{\Lambda}^5\text{He}) = 1.01 \pm 0.20$ MeV. After a re-evaluation in 2010 the separation energy is now given as $\Delta B_{\Lambda\Lambda} = 0.67 \pm 0.17$ MeV [54]. Calculations of the ${}_{\Lambda\Lambda}^6\text{He}$ hypernucleus have been performed in a variety of different approaches such as three-body Faddeev equations applied to the cluster model, in the Brueckner theory approach, or with the stochastic variational method. Those suggest that the $\Lambda\Lambda$ scattering length should be of the order of -1.3 to -0.5 fm [48, 49, 55–61] to obtain separation energies in line with the Nagara event.

Information on the scattering length of two-baryon systems like $\Lambda\Lambda$ can be also extracted from corresponding final-state interactions in production reactions. A method based on dispersion theory that also allows for a quantitative estimation of the theoretical uncertainties has been proposed in Ref. [62]. Its application to available data on the $\Lambda\Lambda$ invariant mass from the reaction ${}^{12}\text{C}(K^-, K^+\Lambda\Lambda X)$ [2] yielded a 1S_0 scattering length of $a = -1.2 \pm 0.6$ fm [52].

Finally, there are constraints for the $\Lambda\Lambda$ scattering length emerging from studies of $\Lambda\Lambda$ correlations in relativistic heavy-ion collisions. In particular, the analysis of Morita et al. [63] of recent data by the STAR collaboration [64] suggests values of $-1.25 < a < -0.56$ fm. It is somewhat disturbing, however, that the experimentalists themselves obtained the rather different value of $a = 1.10 \pm 0.37_{-0.68}^{+0.08}$ fm in their own analysis [64]. Note that a different sign convention is used in that publication.

B. The ΞN system

Results of a measurement of ΞN scattering at low energies have been published by Ahn et al. [44], where upper limits for the $\Xi^- p$ elastic cross section and for $\Xi^- p \rightarrow \Lambda\Lambda$ are given for the p_{Ξ^-} momentum range of 0.2 GeV/c to 0.8 GeV/c. Those limits, 24 mb for the former and 12 mb for the latter, are based on the observation of one event and a null result, respectively. The cross section for $\Xi^- p \rightarrow \Lambda\Lambda$ was also evaluated from three events observed in the reaction ${}^{12}\text{C}(\Xi^-, \Lambda\Lambda)X$ assuming quasi-free scattering and found to be $4.3_{-2.7}^{+6.3}$ mb. A cross section of 4.19 ± 1.9 mb was reported recently by the same group, based on a larger number of events [65]. In an earlier experiment [43] the same collaboration had already deduced the total cross section for $\Xi^- p$ inelastic scattering to be around 13 mb (from nuclear emulsion) and 15 mb (from the Ξ^- absorption probability for ${}^{12}\text{C}$) at $p_{\Xi^-} \simeq 0.6$ GeV/c. Since inelastic scattering involves the reactions $\Xi^- p \rightarrow \Lambda\Lambda$ and $\Xi^- p \rightarrow \Xi^0 n$, the cross-section measurement for the former process mentioned above suggests that $\sigma_{\Xi^- p \rightarrow \Xi^0 n}$ is of the order of 10 mb [44].

In Ref. [45] Aoki et al. reported in-medium results. The inelastic cross section for Ξ^-N in a nucleus was deduced to be $12.7^{+3.5}_{-3.1}$ mb at $p_{\Xi^-} = 0.4 - 0.6$ GeV/c, from a measurement of the quasifree $p(K^-, K^+)\Xi^-$ reaction in nuclear emulsion. The cross section obtained from the number of secondary interactions of Ξ^- particles in the emulsion was estimated to be 20 ± 7 mb. In-medium results have been also presented by Tamagawa et al. [66]. In this publication a Ξ^-N elastic cross section of $30.7 \pm 6.7^{+3.7}_{-3.6}$ mb for an average Ξ momentum of $p_{\Xi} = 550$ MeV/c is reported. Furthermore, the ratio of the Ξ^-p and Ξ^-n scattering cross section was deduced to be $1.1^{+1.4}_{-0.7}{}^{+0.7}_{-0.4}$.

There are also results for ΞN cross sections for various elastic and inelastic channels at Ξ momenta above 1 GeV/c [67–70] from analyses of bubble chamber images. Such momenta are too high to be considered in the present study. However, those data can still serve as qualitative guideline for the trend of the ΞN cross sections with increasing energy. In particular, one does not expect the cross sections around 0.6–1 GeV/c, say, to be significantly larger than the ones observed in those experiments.

Experimental information on the ΞN invariant mass spectrum is scarce [71–73]. In an measurement performed at Saclay [72] the missing mass (MM) in the reaction $K^- + d \rightarrow K^+ + MM$ at 1.4 GeV/c was studied. The curve presented in this publication exhibits a rather smooth behaviour around the ΞN threshold which suggests that the Ξ^-n interaction in the 1S_0 and/or 3S_1 might be fairly weak. Such a conjecture is actually in line with the results of the majority of the potential models which predict rather small Ξ^-n scattering lengths, see Table IV of Ref. [52] for an overview. Also the invariant-mass spectrum published in Ref. [71] for the Ξ^-p case, obtained from a K^-d bubble-chamber experiment, does not show any enhancement near the ΞN threshold. However, the statistics is too low for drawing any solid conclusions.

As already mentioned in the Introduction, an indication for an at least moderately attractive ΞN interaction has been seen in the observed spectrum of the (K^-, K^+) reaction on a ^{12}C target [24]. Here an initial theoretical analysis pointed to an attractive Ξ single particle (s.p.) potential of $U_{\Xi}(p_{\Xi} = 0) \approx -14$ MeV. However, in a re-analysis Kohno et al. [25] came to the conclusion that an almost zero s.p. potential is preferable. Indeed, the in-medium calculation reported in Ref. [26], based on our LO ΞN interaction [29], yields $U_{\Xi}(0) \approx +6$ MeV at nuclear matter saturation density ($k_F = 1.35 \text{ fm}^{-1}$) and could be still compatible with the experiment, judging from the various curves presented in [25]. See also the related work [74] by the same authors. Another facet to this somewhat controversial situation was added by the first evidence for the existence of a deeply bound Ξ^- - ^{14}N system reported in Ref. [27].

III. CHIRAL POTENTIAL AT NEXT-TO-LEADING ORDER

A. General structure

The chiral interaction at NLO consists of BB contact terms without derivatives and with two derivatives, together with contributions from one-pseudoscalar-meson exchanges and from (irreducible) two-pseudoscalar-meson exchanges [40]. The derivation of the baryon-baryon potentials for strangeness in SU(3) chiral EFT up to NLO is described in detail in Refs. [40, 75]. Specifically, the contact terms are discussed in Sect. 2 of Ref. [40] (see also Ref. [75]) together with the one-pseudoscalar-meson exchange potential, while the various contributions from two-pseudoscalar-meson exchange are documented in Appendix A of Ref. [40]. Since the spin-momentum structure is the same for the YN and YY systems we do not reproduce the pertinent expressions here. The only difference occurs in the SU(3) (and isospin) structure and, therefore, we focus just on this aspect. With regard to the contact terms the potentials in the various channels are again of the generic form [40]

$$V = \tilde{C} + C(p^2 + p'^2) \text{ (for } S \text{ waves), } \quad V = Cpp' \text{ (for } P \text{ waves),} \quad (1)$$

etc., but the C 's are now given by different combinations of the basic set of LECs that correspond to the irreducible SU(3) representations $8 \otimes 8 = 27 \oplus 10^* \oplus 10 \oplus 8_s \oplus 8_a \oplus 1$, relevant for scattering of two octet baryons [76, 77]. The pertinent relations are summarized in Table I. For convenience and orientation those for the strangeness $S = 0$ (NN) and $S = -1$ ($\Lambda N, \Sigma N$) are listed, too. The quantities p and p' in Eq. (1) denote the center-of-mass momenta in the initial and final BB states.

The contributions from meson exchange result from taking the appropriate spin-momentum structure given in Ref. [40], and multiplying it with the corresponding combination of baryon-baryon-meson coupling constants and with the isospin factors. Under the assumption that the coupling constants fulfill the standard SU(3) relations the contributions from one- and two-meson exchanges do not involve any free parameters. The relations between the coupling constants, expressed in terms of the axial coupling constant g_A , the pion decay constant f_{π} , and the so-called $F/(F+D)$ -ratio, can be found in Appendix A. Furthermore, we provide there the isospin factors for all single and two-meson exchange diagrams that arise in the strangeness $S = -2$ sector. See also Refs. [29, 40, 75, 78].

TABLE I. SU(3) relations for the various contact potentials in the isospin basis. C_ξ^{27} etc. refers to the corresponding irreducible SU(3) representation for a particular partial wave ξ . The isospin is denoted by I . The actual potential still needs to be multiplied by pertinent powers of the momenta p and p' , see Eq. (1).

		Channel	I	$V(\xi)$			
				$\xi = {}^1S_0, {}^3P_0, {}^3P_1, {}^3P_2$	$\xi = {}^3S_1, {}^3S_1\text{-}{}^3D_1, {}^1P_1$	$\xi = {}^1P_1 \rightarrow {}^3P_1$	$\xi = {}^3P_1 \rightarrow {}^1P_1$
$S = 0$	$NN \rightarrow NN$	$NN \rightarrow NN$	0	–	$C_\xi^{10^*}$	–	–
	$NN \rightarrow NN$	$NN \rightarrow NN$	1	C_ξ^{27}	–	–	–
$S = -1$	$\Lambda N \rightarrow \Lambda N$	$\Lambda N \rightarrow \Lambda N$	$\frac{1}{2}$	$\frac{1}{10} (9C_\xi^{27} + C_\xi^{8_s})$	$\frac{1}{2} (C_\xi^{8_a} + C_\xi^{10^*})$	$-C_\xi^{8_{sa}}$	$-C_\xi^{8_{sa}}$
	$\Lambda N \rightarrow \Sigma N$	$\Lambda N \rightarrow \Sigma N$	$\frac{1}{2}$	$\frac{3}{10} (-C_\xi^{27} + C_\xi^{8_s})$	$\frac{1}{2} (-C_\xi^{8_a} + C_\xi^{10^*})$	$-3C_\xi^{8_{sa}}$	$C_\xi^{8_{sa}}$
	$\Sigma N \rightarrow \Sigma N$	$\Sigma N \rightarrow \Sigma N$	$\frac{1}{2}$	$\frac{1}{10} (C_\xi^{27} + 9C_\xi^{8_s})$	$\frac{1}{2} (C_\xi^{8_a} + C_\xi^{10^*})$	$3C_\xi^{8_{sa}}$	$3C_\xi^{8_{sa}}$
	$\Sigma N \rightarrow \Sigma N$	$\Sigma N \rightarrow \Sigma N$	$\frac{3}{2}$	C_ξ^{27}	C_ξ^{10}	–	–
$S = -2$	$\Lambda\Lambda \rightarrow \Lambda\Lambda$	$\Lambda\Lambda \rightarrow \Lambda\Lambda$	0	$\frac{1}{40} (27C_\xi^{27} + 8C_\xi^{8_s} + 5C_\xi^{1_\xi})$	–	–	–
	$\Lambda\Lambda \rightarrow \Xi N$	$\Lambda\Lambda \rightarrow \Xi N$	0	$\frac{-1}{40} (18C_\xi^{27} - 8C_\xi^{8_s} - 10C_\xi^{1_\xi})$	–	–	$2C_\xi^{8_{sa}}$
	$\Lambda\Lambda \rightarrow \Sigma\Sigma$	$\Lambda\Lambda \rightarrow \Sigma\Sigma$	0	$\frac{\sqrt{3}}{40} (-3C_\xi^{27} + 8C_\xi^{8_s} - 5C_\xi^{1_\xi})$	–	–	–
	$\Xi N \rightarrow \Xi N$	$\Xi N \rightarrow \Xi N$	0	$\frac{1}{40} (12C_\xi^{27} + 8C_\xi^{8_s} + 20C_\xi^{1_\xi})$	$C_\xi^{8_a}$	$2C_\xi^{8_{sa}}$	$2C_\xi^{8_{sa}}$
	$\Xi N \rightarrow \Sigma\Sigma$	$\Xi N \rightarrow \Sigma\Sigma$	0	$\frac{\sqrt{3}}{40} (2C_\xi^{27} + 8C_\xi^{8_s} - 10C_\xi^{1_\xi})$	–	$2\sqrt{3}C_\xi^{8_{sa}}$	–
	$\Sigma\Sigma \rightarrow \Sigma\Sigma$	$\Sigma\Sigma \rightarrow \Sigma\Sigma$	0	$\frac{1}{40} (C_\xi^{27} + 24C_\xi^{8_s} + 15C_\xi^{1_\xi})$	–	–	–
	$\Xi N \rightarrow \Xi N$	$\Xi N \rightarrow \Xi N$	1	$\frac{1}{5} (2C_\xi^{27} + 3C_\xi^{8_s})$	$\frac{1}{3} (C_\xi^{10} + C_\xi^{10^*} + C_\xi^{8_a})$	$-2C_\xi^{8_{sa}}$	$-2C_\xi^{8_{sa}}$
	$\Xi N \rightarrow \Sigma\Lambda$	$\Xi N \rightarrow \Sigma\Lambda$	1	$\frac{\sqrt{6}}{5} (C_\xi^{27} - C_\xi^{8_s})$	$\frac{\sqrt{6}}{6} (C_\xi^{10} - C_\xi^{10^*})$	$\sqrt{\frac{8}{3}}C_\xi^{8_{sa}}$	–
	$\Xi N \rightarrow \Sigma\Sigma$	$\Xi N \rightarrow \Sigma\Sigma$	1	–	$\frac{\sqrt{2}}{6} (C_\xi^{10} + C_\xi^{10^*} - 2C_\xi^{8_a})$	–	$2\sqrt{2}C_\xi^{8_{sa}}$
	$\Sigma\Lambda \rightarrow \Sigma\Lambda$	$\Sigma\Lambda \rightarrow \Sigma\Lambda$	1	$\frac{1}{5} (3C_\xi^{27} + 2C_\xi^{8_s})$	$\frac{1}{2} (C_\xi^{10} + C_\xi^{10^*})$	–	–
	$\Sigma\Lambda \rightarrow \Sigma\Sigma$	$\Sigma\Lambda \rightarrow \Sigma\Sigma$	1	–	$\frac{\sqrt{3}}{6} (C_\xi^{10} - C_\xi^{10^*})$	–	$\frac{4}{\sqrt{3}}C_\xi^{8_{sa}}$
	$\Sigma\Sigma \rightarrow \Sigma\Sigma$	$\Sigma\Sigma \rightarrow \Sigma\Sigma$	1	–	$\frac{1}{6} (C_\xi^{10} + C_\xi^{10^*} + 4C_\xi^{8_a})$	–	–
	$\Sigma\Sigma \rightarrow \Sigma\Sigma$	$\Sigma\Sigma \rightarrow \Sigma\Sigma$	2	C_ξ^{27}	–	–	–

Once the potentials are established, a partial-wave projection of them is performed, as described in detail in Ref. [39]. The reaction amplitudes are obtained from the solution of a coupled-channel Lippmann-Schwinger (LS) equation:

$$T_{\nu''\nu'}^{\rho''\rho',J}(p'',p';\sqrt{s}) = V_{\nu''\nu'}^{\rho''\rho',J}(p'',p') + \sum_{\rho,\nu} \int_0^\infty \frac{dpp^2}{(2\pi)^3} V_{\nu''\nu'}^{\rho''\rho',J}(p'',p) \frac{2\mu_\nu}{q_\nu^2 - p^2 + i\eta} T_{\nu\nu'}^{\rho\rho',J}(p,p';\sqrt{s}). \quad (2)$$

Here, the label ν indicates the particle channels and the label ρ the partial wave. μ_ν is the pertinent reduced baryon mass. The on-shell momentum q_ν in the intermediate state, is determined by $\sqrt{s} = \sqrt{M_{B_{1,\nu}}^2 + q_\nu^2} + \sqrt{M_{B_{2,\nu}}^2 + q_\nu^2}$. Relativistic kinematics is used for relating the laboratory momentum p_{lab} of the hyperons to the center-of-mass momentum.

We solve the LS equation in the particle basis, in order to incorporate the correct physical thresholds. This is important for the channels with total charge zero where the relatively large mass difference of around 7 MeV between the Ξ^0 and Ξ^- [79] causes a corresponding splitting between the $\Xi^0 n$ and $\Xi^- p$ thresholds. Depending on the total charge, up to six baryon-baryon channels can couple. The Coulomb interaction is not taken into account in the present study because there are simply no near-threshold data that would require such a more elaborate treatment. The potentials in the LS equation are cut off with a regulator function, $f_R(\Lambda) = \exp[-(p'^4 + p^4)/\Lambda^4]$, in order to remove high-energy components [32]. We consider cut-off values of $\Lambda = 500 - 650$ MeV, i.e. in that range where the best results were achieved in our study of the ΛN and ΣN interactions [40]. Accordingly, we display our results as bands which represent their variation with the cut-off. Note that similar Λ values are also used for chiral NN potentials [32]. As discussed later, this cut-off variations gives only a rough estimate of the theoretical uncertainty.

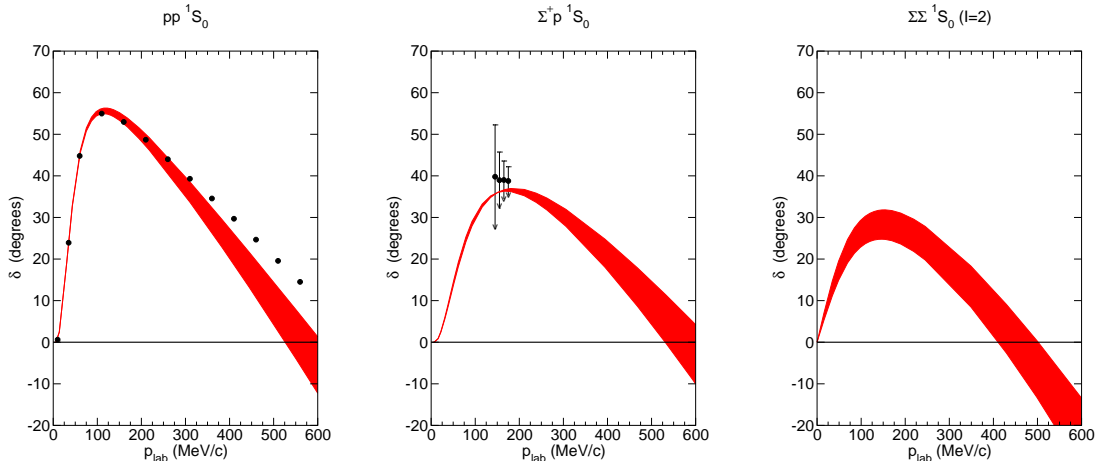


FIG. 2. pp , Σ^+p , and $\Sigma^+\Sigma^+$ phase shifts in the 1S_0 partial wave. The filled band represent our results at NLO. The pp phase shifts of the GWU analysis [80] are shown by circles. In case of Σ^+p the circles indicate upper limits for the phase shifts, deduced from the Σ^+p cross section [78]. The results are taken over from Ref. [78].

B. Determination of contact terms

In our EFT study of the YN interaction [40] we were able to determine practically all contact terms (at least for the S waves) by a direct fit to the pertinent ΛN and ΣN data, without any recourse to the NN system. This is not possible for the $S = -2$ sector due to the already mentioned limited experimental information. Here, in general, we will and have to take over the LECs fixed in our fit to the YN data before. In principle, this is required by a rigorous implementation of $SU(3)$ symmetry anyway.

Having said this, we want to recall that in Ref. [40] it had turned out that a simultaneous description of the YN data and the NN phase shifts is not possible if one really insists on consistent and strictly $SU(3)$ symmetric contact terms. In particular, the value of the contact term $\tilde{C}_{1S_0}^{27}$, required for reproducing the pp (or np) 1S_0 phase shifts on the one hand and for describing the Σ^+p cross section on the other hand could not be reconciled with the requirements of complete $SU(3)$ symmetry given by the relations in Table I. In the light of this observation, in the present study we will also depart from the strict $SU(3)$ connection with the YN sector in cases where we see a strong indication for that from the comparison of our results with the $S = -2$ data. In practice this concerns the LECs $\tilde{C}_{1S_0}^{27}$ and $\tilde{C}_{3S_1}^{8_a}$.

Before we discuss the details, let us emphasize that this policy is consistent with the employed power counting scheme. At NLO $SU(3)$ symmetry breaking in the leading S -wave contact terms arises already naturally in the perturbative expansion of the baryon-baryon potential due to meson mass insertions [75]. Actually, this aspect was exploited by us in a recent study [78]. For the 1S_0 partial wave and for BB channels with maximal isospin there is only one independent $SU(3)$ symmetry breaking LEC for the $S = 0, -1$, and -2 systems, i.e.

$$\begin{aligned}
 V_{NN}^{(I=1)} &= \tilde{C}_{1S_0}^{27} + C_{1S_0}^{27}(p^2 + p'^2) + \frac{1}{2}C_1^\chi(m_K^2 - m_\pi^2), \\
 V_{\Sigma N}^{(I=3/2)} &= \tilde{C}_{1S_0}^{27} + C_{1S_0}^{27}(p^2 + p'^2) + \frac{1}{4}C_1^\chi(m_K^2 - m_\pi^2), \\
 V_{\Sigma\Sigma}^{(I=2)} &= \tilde{C}_{1S_0}^{27} + C_{1S_0}^{27}(p^2 + p'^2),
 \end{aligned} \tag{3}$$

in the notation used in Ref. [78]. The aforementioned pp phase shifts and the Σ^+p cross section can be used to pin down the symmetry breaking LEC C_1^χ together with $\tilde{C}_{1S_0}^{27}$ and $C_{1S_0}^{27}$ and, therefore, we could give predictions for the $\Sigma\Sigma$ interaction with isospin $I = 2$. The corresponding phase shifts are shown in Fig. 2.

In the present study we take over the LECs $\tilde{C}_{1S_0}^{27}$ and $C_{1S_0}^{27}$ for the $\Sigma\Sigma$ channel as given in Table 3 of Ref. [78] and use them for all interactions in the 1S_0 partial wave in the $S = -2$ sector. The negative value of the $SU(3)$ breaking term C_1^χ [78] implies that there is a decrease in the attraction when one goes from the NN system to $S = -1$ and then to $S = -2$, see Eq. (3). Accordingly, the $\Lambda\Lambda$ interaction based on $\tilde{C}_{1S_0}^{27}$ and $C_{1S_0}^{27}$ from Ref. [78] is less attractive than if we would have used those determined in a fit to the YN data [40] following strictly $SU(3)$ arguments. For the LECs

$\tilde{C}_{1S_0}^{8_s}$ and $C_{1S_0}^{8_s}$ we adopt the values from our YN study [40]. The interactions in the 1S_0 partial wave in the $I = 0$ channels involve also the LECs \tilde{C}^1 and C^1 which correspond to the 1 irreducible representation, see Table I. Those terms do not contribute to the NN and YN systems. In an attempt to assign values to those LECs we followed our previous study [29] and varied them within limits set roughly by the so-called natural value which is equal to $4\pi/f_\pi^2$ for the LO partial-wave projected contact term [36]. Since the $\Lambda\Lambda$ interaction is expected to be only moderately attractive, as discussed above, we considered only such variations of the C^1 's that led to $\Lambda\Lambda$ scattering lengths in the range of -1 to -0.5 fm. In particular, we excluded regions which resulted in bound states or near-threshold resonances in the $\Lambda\Lambda$ or ΞN systems, for which there is no experimental support at present.

The LECs in the 3S_1 - 3D_1 partial wave are taken over from the YN sector [40]. For that partial wave the symmetry breaking LECs are strongly interrelated [75] and it is impossible to determine any of these by considering the NN phase shifts together with the experimental information on the ΛN and ΣN systems. It turns out that the $S = -2$ BB interaction based on those LECs leads to a $\Xi^- p$ cross section that exceeds the upper limit given in Ref. [44]. The main reason for that is the appearance of a bound state close to the ΞN threshold in the 3S_1 - 3D_1 partial wave with $I = 0$. Since only LECs in the 8_a representation contribute to this channel, see Table I, we simply readjust $\tilde{C}_{3S_1}^{8_a}$ in order to obtain an interaction that yields ΞN results consistent with the experimental bounds. Actually, an inspection of Table 3 in [40] reveals that the values of $\tilde{C}_{3S_1}^{8_a}$ are much much smaller than any of the other LECs. Thus, one could speculate that those values are not so well determined in the fit to the YN data anyway. In practice only a small change in $\tilde{C}_{3S_1}^{8_a}$ is needed to remove the bound state and to achieve ΞN cross sections in line with the bounds suggested by the experiments.

The contact terms in the P waves are all taken over from Ref. [40], with one exception: We readjusted the $C_{1P_1}^{8_a}$ of the YN interaction of [40] so that now the Λp 1P_1 phase shift is overall repulsive. This has no influence on the cross section results presented in Ref. [40]. However, the predicted ΞN cross sections are then smaller at higher momenta and, therefore, better in line with the behavior suggested by the experiments. The values for the C^1 's (occurring in the 3P_0 , 3P_1 , and 3P_2 partial waves) have been likewise fixed by the requirement that the ΞN cross sections should remain small for higher energies. We do not consider 1P_1 - 3P_1 mixing at this stage, i.e. we put $C^{8_{sa}}$ to zero. All low-energy constants used in the present study are tabulated in Appendix A.

While the above strategy allows us to fix all LECs we are certainly far from being able to determine them uniquely, as should have become obvious from the preceding discussion. This is a consequence of the limited experimental information. The situation differs from that in our EFT study of the YN interaction where, as noted, practically all contact terms (at least for the S waves) could be really fixed by a direct fit to ΛN and ΣN data. In view of these circumstances it should be clear that the present investigation on the BB interaction in the $S = -2$ sector, performed in chiral EFT up to NLO, can only have a preliminary and exploratory status.

IV. RESULTS

Let us start with the $\Lambda\Lambda$ and ($I = 2$) $\Sigma\Sigma$ channels which are determined solely by the symmetric SU(3) representations (27, 8_s , 1), see Table I. Corresponding results are displayed in Fig. 3 (cross sections) and summarized in Table II (effective range parameters). As discussed in the preceding section, we use here the LECs $\tilde{C}_{1S_0}^{27}$ and $C_{1S_0}^{27}$ determined in our combined analysis of the pp and $\Sigma^+ p$ systems [78] where SU(3) breaking in the leading term is incorporated. It is reassuring to see that the results based on those LECs are in agreement with the data points as well as with the upper limit for the reaction $\Xi^- p \rightarrow \Lambda\Lambda$ provided in Refs. [44, 65], see the black (red) band in Fig. 3. In addition, the $\Lambda\Lambda$ 1S_0 scattering length is well within the range implied by studies of bound states and reactions involving the $\Lambda\Lambda$ interaction summarized in Sect. II.A. For the LECs in the SU(3) singlet representation, $\tilde{C}_{1S_0}^1$ and $C_{1S_0}^1$, values close to zero had to be chosen. Any somewhat larger positive values lead to scattering lengths smaller than -0.5 fm while negative values would result in a H -dibaryon like near-threshold bound state in the ΞN system. If one takes over the values for the C^{27} 's from the YN fit [40] then the $\Lambda\Lambda$ scattering length would be in the order of -2 fm, i.e. clearly too large in view of the aforementioned analyses. It turned out that it is not possible to achieve a reduction from -2 fm, say, to the preferred range of -0.5 to -1 fm by a variation of the LECs $\tilde{C}_{1S_0}^1$ and $C_{1S_0}^1$ within its natural range.

One can see from Fig. 3 that already the result at LO was consistent with the data for $\Xi^- p \rightarrow \Lambda\Lambda$ (grey/green band). On the other hand, the $\Lambda\Lambda$ scattering length might be somewhat too large based on the expectations discussed above.

The ΞN interaction involves contributions from symmetric and antisymmetric SU(3) representations, see Table I. Results for $\Xi^- p$ elastic and inelastic cross sections and for the charge exchange reaction $\Xi^- p \rightarrow \Xi^0 n$ are displayed in Fig. 4. The black (red) bands represent those of our NLO interaction based on the re-adjusted leading contact term $\tilde{C}_{3S_1}^{8_a}$, cf. the discussion in Sect. III.B. Obviously, a nice agreement with the empirical information on the inelastic and charge-exchange cross sections is achieved and, moreover, the limits set by the measurement of Ahn et al. [44] for $\Xi^- p$

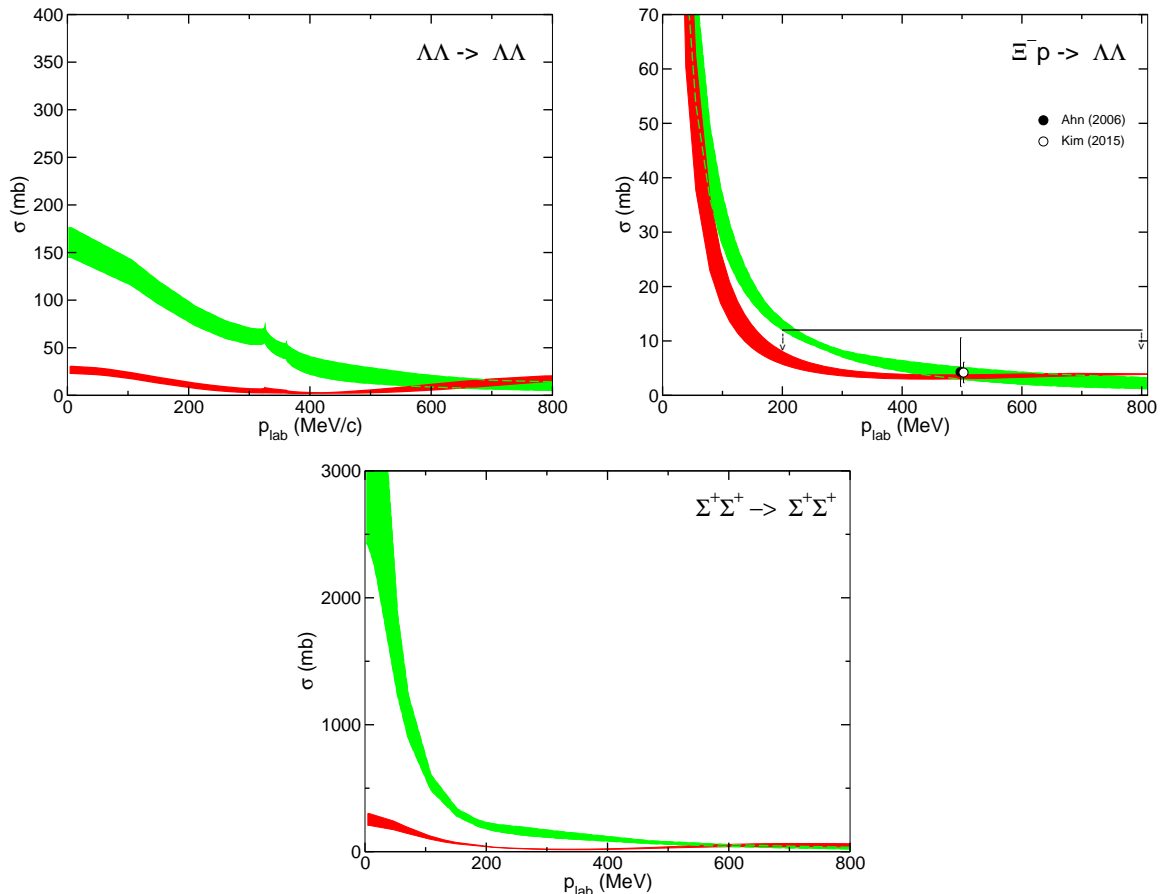


FIG. 3. $\Lambda\Lambda$ and $\Sigma^+\Sigma^+$ cross sections. The bands represent our results at NLO (black/red) and LO (grey/green). The experimental information is taken from Ahn et al. [44] (filled circle) and Kim [65] (open circle). Upper limits are indicated by arrows.

TABLE II. Scattering lengths and effective ranges (in fm) for $\Lambda\Lambda$ and $\Sigma^+\Sigma^+$, for various cut-off values (in MeV).

Λ		NLO				LO			
		500	550	600	650	550	600	650	700
$\Lambda\Lambda$	a_{1S0}	-0.62	-0.61	-0.66	-0.70	-1.52	-1.52	-1.54	-1.67
	r_{1S0}	6.95	6.06	5.05	4.56	0.82	0.59	0.31	0.34
$\Sigma^+\Sigma^+$	a_{1S0}	-2.19	-1.94	-1.83	-1.82	-6.23	-7.76	-9.42	-9.27
	r_{1S0}	5.67	5.97	6.05	5.93	2.17	2.00	1.88	1.88

elastic scattering are also strictly fulfilled. Note that the inelastic cross section reported in Ref. [45] is actually for Ξ^-N . However, the first inelastic channel for Ξ^-n , namely $\Lambda\Sigma^-$, opens around $p_{\Xi^-} = 590$ MeV/c in free scattering, i.e. practically above the momentum range covered by the experiment. Therefore, it is sensible to compare this data point with our Ξ^-p results.

For illustration purposes we display also results where all LECs in the antisymmetric SU(3) representations (10^* , 10 , 8_a) were taken over from the YN fit [40]. Evidently, in this case the Ξ^-p cross sections (hatched bands) are too large as compared to the experiments. Specifically, the charge-exchange as well as the inelastic cross section are overestimated by roughly a factor two. Though the data in question come from in-medium measurements [44, 45] it is unrealistic to assume that medium effects could explain the observed discrepancy. Indeed, at Ξ momenta around 500 MeV/c one would expect that such effects are moderate, say in the order of 10 % or at most 20 %, as suggested by corresponding calculations for the NN system [81–83].

Interestingly, the results based on our LO interaction from Ref. [29] (grey/green bands) are consistent with all

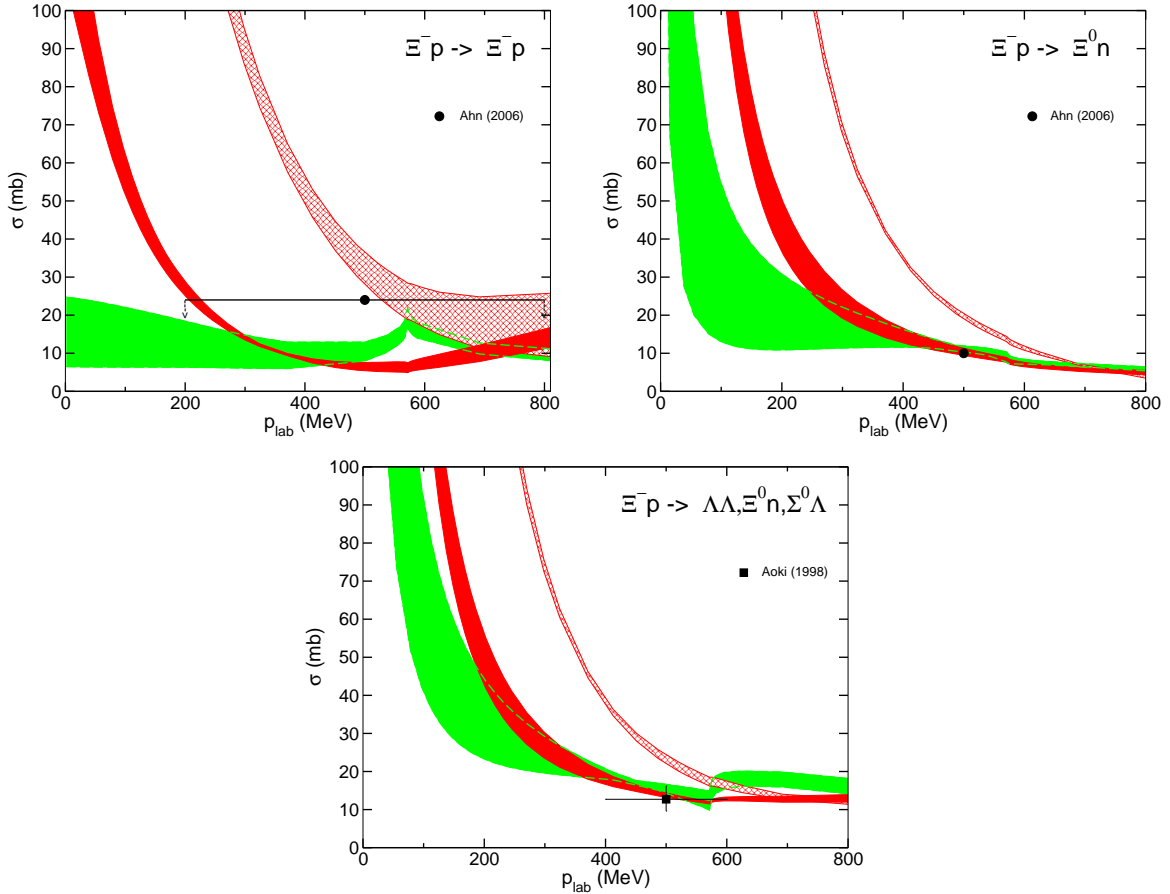


FIG. 4. $\Xi^- p$ induced cross sections. The bands represent our results at NLO (black/red) and LO (grey/green). The hatched band shows results based on \tilde{C}_{3,S_1}^{8a} from Ref. [40], see text. Experiments are from Ahn et al. [44] and Aoki et al. [45]. Upper limits are indicated by arrows.

empirical constraints. Those cross sections are basically genuine predictions that follow from SU(3) symmetry utilizing LECs fixed from a fit to the ΛN and ΣN data on the LO level. The LO calculation exhibits also a sizeable cusp effect in the $\Xi^- p$ cross sections at the opening of the $\Lambda\Sigma^0$ threshold which indicates a strong coupling to this channel. This effect is much smaller for our NLO interaction and barely visible on the scale of Fig. 4.

The $\Xi^0 p$ system is a pure isospin $I = 1$ state. Predictions for $\Xi^0 p$ induced reactions are displayed in Fig. 5. There are no data for the $\Xi^0 p$ channel in the momentum region up to 1 GeV/c. The NLO and LO results for $\Xi^0 p$ elastic scattering are of comparable order of magnitude. Like before for $\Xi^- p$, employing the LEC \tilde{C}_{3,S_1}^{8a} from the YN sector leads to a stronger interaction and would imply a much larger $\Xi^0 p$ cross section near threshold (hatched band). Again the cusp effect (now at the $\Lambda\Sigma^+$ threshold) is strongly reduced for the NLO interaction. Data at higher momenta suggest a $\Xi^0 p$ elastic cross section in the order of 10 to 30 mb [67, 68]. Tamagawa et al. have deduced the $\Xi^- N$ elastic cross section and also the ratio of the $\Xi^- p$ to $\Xi^- n$ scattering cross section for an average Ξ momentum of 550 MeV/c [66]. $\Xi^- n$ is like $\Xi^0 p$ a pure $I = 1$ state so that $\sigma_{\Xi^- n} \cong \sigma_{\Xi^0 p}$. Thus, we conclude from Figs. 4 and 5 that our results are compatible with their measurement. Specifically, we get $\sigma_{\Xi^- p}/\sigma_{\Xi^- n} \cong \sigma_{\Xi^- p}/\sigma_{\Xi^0 p} \cong 1$ for $p_{\Xi^-} = 500 \sim 600$ MeV/c as reported in Ref. [66].

The strong coupling between the ΞN and $\Lambda\Sigma$ systems at LO, conjectured from the pronounced cusp in the ΞN cross section, is indeed reflected in the cross section for $\Xi^0 p \rightarrow \Lambda\Sigma^+$. It is significantly larger than the one predicted at NLO, see Fig. 5 (right side). A cross section of 24 mb is given for this transition reaction in Ref. [68] for Ξ 's with an average momentum of 2 GeV/c. The $\Sigma^0\Sigma^+$ channel opens at the Ξ^0 momentum of roughly 970 MeV/c. A value of 6 mb is given for the $\Xi^0 p \rightarrow \Sigma^0\Sigma^+$ transition section in Ref. [68] for Ξ 's with an average momentum of 2 GeV/c. We calculated this cross section for curiosity reasons for our NLO interaction and we found it to be in the order of 1–4 mb for momenta around 1 ~ 1.3 GeV/c.

In general, there is a noticeable reduction of the dependence of the $\Lambda\Lambda$ and $\Xi^- p$ results on the regularization in

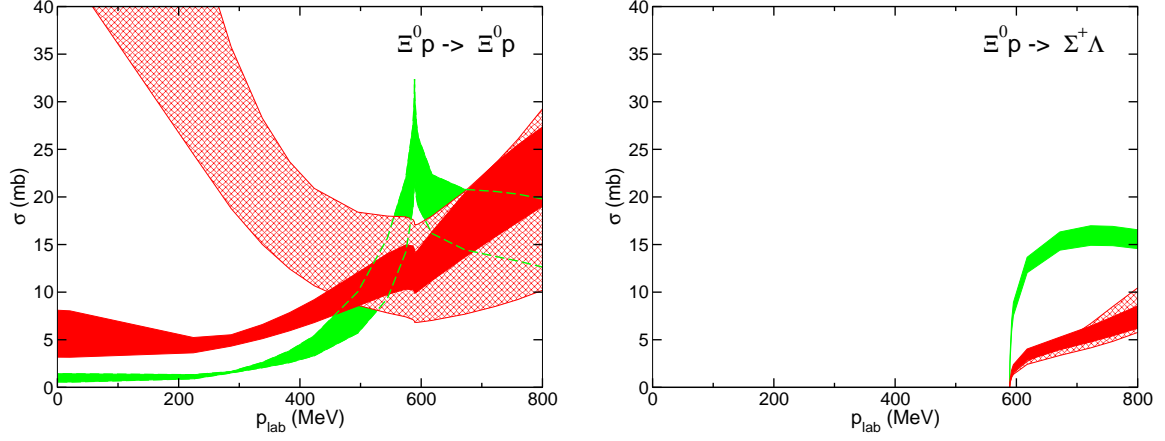


FIG. 5. $\Xi^0 p$ induced cross sections. The bands represent our results at NLO (black/red) and LO (grey/green). The hatched band shows results based on $\tilde{C}_{3S_1}^{S_a}$ from Ref. [40], see text.

TABLE III. Scattering lengths and effective ranges (in fm) for $\Xi^0 p$ and $\Xi^0 n$, for various cut-off values (in MeV). Results for the isospin $I = 0$ ΞN effective range parameters, based on a calculation in isospin basis are also given. (*) indicates the results based on $\tilde{C}_{3S_1}^{S_a}$ from Ref. [40].

Λ		NLO				LO			
		500	550	600	650	550	600	650	700
$I = 0$	a_{3S_1}	-0.33	-0.39	-0.62	-0.85	-0.85	-0.59	-0.43	-0.32
	r_{3S_1}	-6.87	-1.77	1.00	1.42	-1.84	-3.93	-7.16	-12.56
	a_{3S_1} (*)	5.11	4.03	3.97	3.97				
	r_{3S_1} (*)	0.93	1.11	1.24	1.27				
$\Xi^0 p$	a_{1S_0}	0.37	0.39	0.34	0.31	0.21	0.19	0.17	0.13
	r_{1S_0}	-4.71	-4.86	-7.07	-8.99	-30.7	-37.7	-52.8	-98.5
	a_{3S_1}	-0.20	-0.04	0.021	0.039	0.02	0.00	0.02	0.03
	r_{3S_1}	35.6	575.1	1797	450	968	$>10^4$	1166	548
	a_{3S_1} (*)	-1.01	-0.85	-0.72	-0.66				
	r_{3S_1} (*)	3.60	4.04	4.60	4.82				
$\Xi^0 n$	a_{3S_1}	-0.25	-0.20	-0.26	-0.34	-0.34	-0.25	-0.20	-0.15
	r_{3S_1}	5.35	8.36	5.26	2.93	-5.86	-8.27	-4.36	16.3
	a_{3S_1} (*)	11.39	5.15	4.78	4.74				
	r_{3S_1} (*)	-0.37	-0.39	-0.22	-0.18				

our NLO calculation as compared to LO. The cut-off dependence (represented by the bands) provides a lower bound on the theoretical uncertainty and, accordingly, a rough estimate for the latter. It should be said, however, that one cannot expect that the bands resulting from the LO and the NLO interactions overlap for energies close to the threshold, as it is the case in investigations of the NN system [32, 33]. In contrast to NN there are no data at small kinetic energies that pin down the scattering length quantitatively and, as a consequence, the predictions for the cross sections in that region. In fact, the situation for $S = -2$ is similar to the one in our study of the YN system [40] where, for example, also the Λp cross sections at LO and NLO do not overlap close to threshold. Note that recently improved schemes to estimate the theoretical error were proposed and applied to high-order NN results [84–86]. In addition, more efficient regularization schemes than the Gaussian regular function employed in the present study have been advocated [85].

Table III summarizes effective range parameters for the $\Xi^0 p$ and $\Xi^0 n$ channels. Furthermore, ΞN results for $I = 0$ calculated in the isospin basis and using an average Ξ mass of 1318.07 MeV are provided. There is a large difference between the physical masses of the Ξ^0 and Ξ^- [79] which causes a noticeable isospin breaking in the ΞN system in the

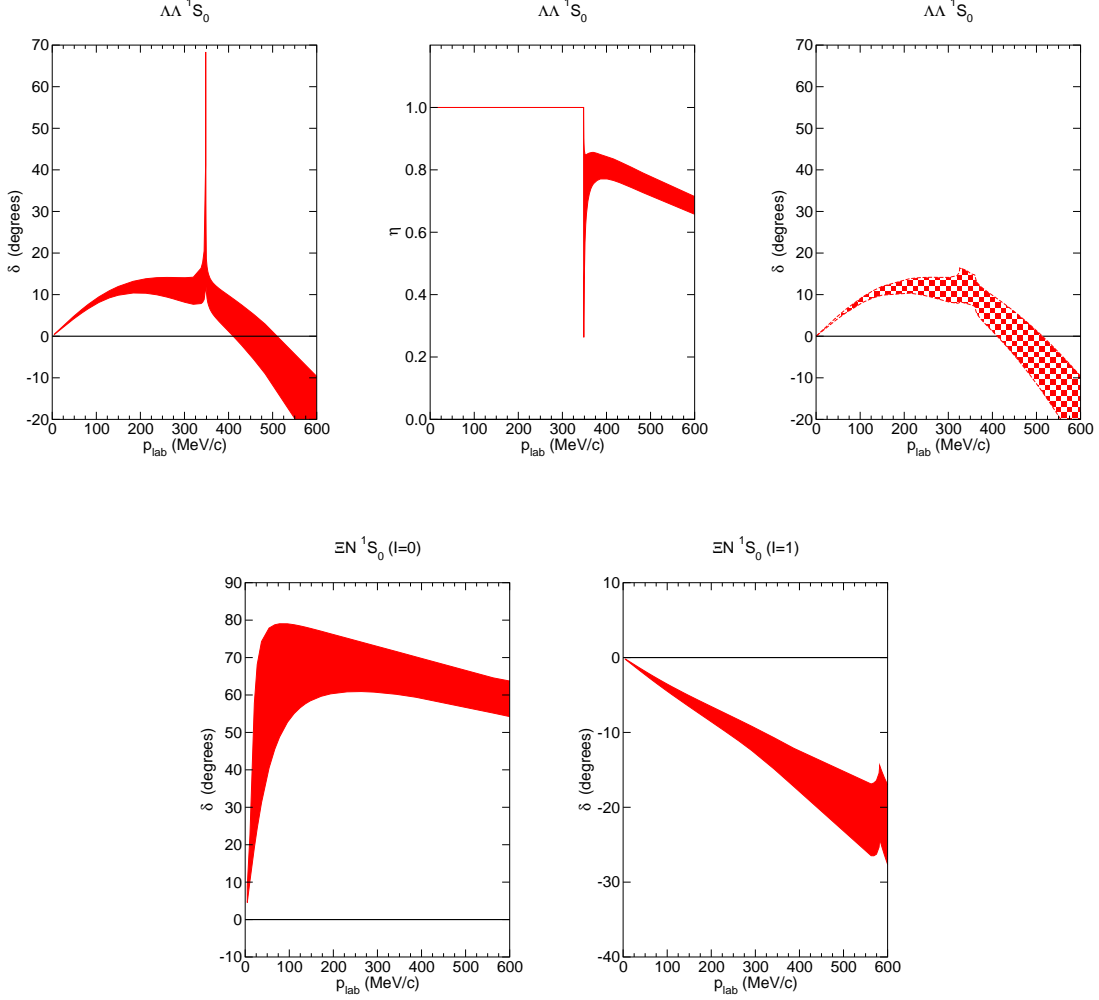


FIG. 6. $\Lambda\Lambda$ and ΞN phase shifts in the 1S_0 partial wave calculated in isospin basis. η is defined by $S = \eta e^{2i\delta}$. The bands represent our results at NLO. The panel on the upper right side shows the result for $\Lambda\Lambda$ obtained in the particle basis.

threshold region because the thresholds for the $\Xi^0 n$ and $\Xi^- p$ channels do not coincide (as they would in the isospin symmetric case) but are separated by about 7 MeV. On the other hand, the results for $I = 1$ (based on averaged Ξ and N masses) are very close to those for $\Xi^0 p$ and, therefore, we do not write them down separately.

We list only effective range parameters for elastic channels. Thus, for isospin $I = 0$ only results for the 3S_1 partial wave are given because in this case there is no coupling of ΞN to $\Lambda\Lambda$ due to the Pauli principle. One can see from Table III that the NLO and LO potentials yield $I = 0$ scattering lengths of comparable magnitude. In both cases a weakly attractive interaction is predicted. Also the cut-off dependence is comparable, though its effect is actually reversed at NLO as compared to the LO case. The NLO interaction based on the value of $\tilde{C}_{^3S_1}^{8a}$ from Ref. [40] is much more attractive, see the results marked with an asterisk (*) in Table III. Indeed, the large and positive scattering length predicted here is in the order of the one in the np 3S_1 partial wave where there is a bound state, namely the deuteron. Thus, connecting YN and ΞN by strict $SU(3)$ symmetry would imply the existence of a deuteron-like state in the $I = 0$ ΞN system for our NLO interaction. However, as argued above, with such a strongly attractive force we are not able to meet the constraints set by the experiments. Hence, if one takes those constraints serious one would rather exclude the existence of such a state.

The effective range parameters for $\Xi^0 p$ reveal that the interaction in the isospin $I = 1$ channel is likewise weak. The small and positive values of the scattering length in the 1S_0 partial wave point to a weak repulsion. Again the results obtained at the NLO and LO level are comparable. With regard to the results for the 3S_1 partial wave based on $\tilde{C}_{^3S_1}^{8a}$ from Ref. [40] those are somewhat more attractive but there is no dramatic difference. In some cases, notably

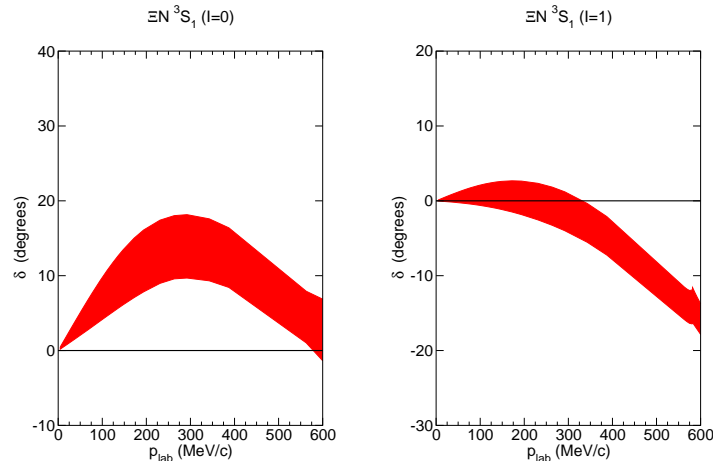


FIG. 7. ΞN phase shifts in the 3S_1 partial wave calculated in isospin basis. The bands represent our results at NLO.

in the 3S_1 partial wave, we observe unnaturally large values for the effective range, which is clearly related to the strong suppression of the corresponding scattering length. This peculiarity occurs also in phenomenological models of the BB interaction [47, 49, 52].

When isospin symmetry is fulfilled then the $\Xi^0 n$ scattering length is given simply by $(a^{I=0} + a^{I=1})/2$. However, as mentioned above, the large splitting between the Ξ^0 and Ξ^- masses causes a sizeable isospin breaking in the reaction amplitudes when solving the coupled-channels LS equation (2) in the particle basis, see the actual results for $\Xi^0 n$ in Table III. A striking isospin breaking effect occurs in the NLO interaction with $\tilde{C}_{3S_1}^{8_a}$ from Ref. [40] due to the presence of the near-threshold deuteron-like bound state. This state is now even closer to the threshold, as testified by the increase in the scattering length as compared to the $I = 0$ case for all cut-off values.

Finally, for completeness, in Figs. 6 and 7 we present phase shifts for the $\Lambda\Lambda$ and ΞN 1S_0 and 3S_1 partial waves for $I = 0$ and 1, calculated in the isospin basis employing isospin-averaged masses. In addition, the inelasticity parameter η (based on the standard parametrization of the S -matrix, $S = \eta e^{2i\delta}$) is shown for the coupled system $\Lambda\Lambda - \Xi N - \Sigma\Sigma$ in the $I = 0$ channel. Results for the $\Sigma\Sigma$ channel with $I = 2$ can be found in Fig. 2.

The most interesting feature in the phase-shift results is certainly the spectacular cusp that occurs in the $\Lambda\Lambda$ system at the opening of the ΞN channel. It is the consequence of an inelastic virtual state [87] very close to the ΞN threshold predicted by the NLO interaction. This state can be seen as a remnant of the H -dibaryon. Indeed, some extrapolations of the lattice QCD results indicate that the dibaryon could be actually located close to the ΞN threshold, see Refs. [10, 11] and the $\Lambda\Lambda$ phase shifts presented in those works. A structure close to the ΞN threshold is also predicted by the quark-model based BB interaction FSS in Ref. [49]. Concerning our results it should be said, however, that there is a drastical change when we perform the same calculation in particle basis. Then the $\Xi^0 n$ and $\Xi^- p$ channels open at different energies and, in particular, the virtual state is farther away from the lower threshold (the one of $\Xi^0 n$). Accordingly, in this case there are two cusps and both are rather modest, see the panel on the right hand side of Fig. 6. This is also manifest in the corresponding cross section (cf. Fig. 3) where the opening of the ΞN channels is barely visible. Cusps appear also in the ΞN $I = 1$ phase shifts at the opening of the $\Sigma\Lambda$ channel, in the 1S_0 as well as in the 3S_1 partial waves.

For $I = 0$ chiral EFT at NLO predicts positive values for both S -wave phase shifts, which signals an attractive ΞN force in that isospin channel, cf. also the discussion on the scattering lengths above. The phase shift in the 1S_0 partial wave is rather large as a result of the presence of the aforementioned virtual state. In case of $I = 1$ the phase shifts are predominantly negative and, accordingly, the ΞN force essentially repulsive. It should be mentioned that qualitatively similar features have been reported in Ref. [49] for a BB interaction derived in the quark model.

V. SUMMARY

In this paper we presented a potential for the baryon-baryon interaction in the strangeness $S = -2$ sector, derived in chiral effective field theory to next-to-leading order in the Weinberg counting. At the considered order there are contributions from one- and two-pseudoscalar-meson exchange diagrams and from four-baryon contact terms without

and with two derivatives. As in case of our study to the ΛN and ΣN systems [40], SU(3) flavor symmetry is used as guiding principle in the derivation of the interaction. This means that all the coupling constants at the various baryon-baryon-meson and baryon-baryon-meson-meson vertices are fixed from SU(3) symmetry and the symmetry is also exploited to derive relations between the contact terms. Furthermore, contributions from all mesons of the pseudoscalar octet (π , K , η) are taken into account. The SU(3) symmetry is, however, broken by the masses of the pseudoscalar mesons and of the baryons for which we take the known physical values.

In the application of this scheme to the $S = -1$ sector we found that one can achieve a combined description of the ΛN and ΣN systems without any explicit SU(3) breaking in the contact interactions. However, it also turned out that a simultaneous description of the YN data and the NN interaction, with contact terms fulfilling SU(3) symmetry strictly and consistently, is not possible. Specifically, the strength of the contact interaction in the 27-representation that is needed to reproduce the pp (or np) 1S_0 phase shifts is simply not compatible with the one required for the description of the empirical Σ^+p cross section [40]. The same observation is now made in the extension to $S = -2$. Also here we cannot simply take over all the low-energy constants as fixed from fitting to the ΛN and ΣN data. If we want to satisfy the limited and mostly qualitative experimental constraints on the $\Lambda\Lambda$ and ΞN systems then some of the LECs need to be re-adjusted. We want to emphasize that an SU(3) breaking in the leading S -wave contact terms is in line with the employed power counting scheme [75] and with the results published in Ref. [78].

Our results suggest that the ΞN interaction has to be relatively weak in order to be in accordance with the available empirical constraints. In particular, the published values and upper bounds for the Ξ^-p elastic and inelastic cross sections [44, 45, 65] practically rule out a somewhat stronger attractive ΞN force and, specifically, disfavors any near-threshold deuteron-like bound states in that system. However, it remains to be seen in how far such a weakly attractive ΞN interaction is in line with other experimental evidence such as a recently reported deeply bound Ξ hypernucleus [27]. It should be also mentioned that the latest and still preliminary results from lattice QCD simulations apparently suggest a somewhat more attractive ΞN interaction [88], notably in the 3S_1 partial wave with isospin $I = 0$ [89].

In any case, we want to emphasize that the present investigation, performed in chiral EFT up to NLO, should be considered to be of preliminary and exploratory nature. While in our preceding study for the ΛN and ΣN interactions we were able to fix practically all pertinent contact terms (at least for the S waves) by a direct fit to corresponding data, without any recourse to the NN system, this is not possible for the strangeness $S = -2$ sector. Here we are not in a position that would allow us to determine the relevant LECs uniquely, due to the rather limited empirical information. Planned experimental efforts at sites like J-PARC [90] in Japan and/or FAIR [91, 92] in Darmstadt will hopefully lead to an appreciable improvement of the data base in the not too far future and, thus, provide important further constraints on the strangeness $S = -2$ baryon-baryon interaction.

ACKNOWLEDGMENTS

We thank Norbert Kaiser and Wolfram Weise for useful discussions. This work is supported in part by the DFG and the NSFC through funds provided to the Sino-German CRC 110 ‘‘Symmetries and the Emergence of Structure in QCD’’. S. Petschauer thanks the ‘‘TUM Graduate School’’. Part of the numerical calculations has been performed on the supercomputer cluster of the JSC, Jülich, Germany.

Appendix A: Coupling constants and isospin factors

For a baryon-baryon-meson interaction Lagrangian that is SU(3)-invariant the various coupling constants are related with each other by [76]

$$\begin{aligned}
 f_{NN\pi} &= f, & f_{NN\eta_8} &= \frac{1}{\sqrt{3}}(4\alpha - 1)f, & f_{\Lambda NK} &= -\frac{1}{\sqrt{3}}(1 + 2\alpha)f, \\
 f_{\Xi\Xi\pi} &= -(1 - 2\alpha)f, & f_{\Xi\Xi\eta_8} &= -\frac{1}{\sqrt{3}}(1 + 2\alpha)f, & f_{\Xi\Lambda K} &= \frac{1}{\sqrt{3}}(4\alpha - 1)f, \\
 f_{\Lambda\Sigma\pi} &= \frac{2}{\sqrt{3}}(1 - \alpha)f, & f_{\Sigma\Sigma\eta_8} &= \frac{2}{\sqrt{3}}(1 - \alpha)f, & f_{\Sigma NK} &= (1 - 2\alpha)f, \\
 f_{\Sigma\Sigma\pi} &= 2\alpha f, & f_{\Lambda\Lambda\eta_8} &= -\frac{2}{\sqrt{3}}(1 - \alpha)f, & f_{\Xi\Sigma K} &= -f.
 \end{aligned}
 \tag{A1}$$

Thus, all coupling constants are given in terms of $f \equiv g_A/2f_0$ and the ratio $\alpha = F/(F + D)$. We use the values $g_A = 1.26$ for the axial coupling constant and $f_0 \approx f_\pi = 93$ MeV for the pion decay constant, while for the so-called $F/(F + D)$ -ratio we adopt the SU(6) value $\alpha = 0.4$. The η meson is identified with the octet-state η_8 . In principle, there is an explicit SU(3) symmetry breaking in the coupling constants as reflected in the different empirical values of the decay constants f_π , f_K and f_η [79], which we ignored in [40] and will do so also in the present work. The only

TABLE IV. Isospin factors for the various one-pseudoscalar-meson exchanges. P_f is the flavor-exchange operator, and $P_+ = (1 + P_f)/2$, $P_- = (1 - P_f)/2$.

Channel	Isospin	π	K	η
$\Lambda\Lambda \rightarrow \Lambda\Lambda$	0	0	0	P_+
$\Lambda\Lambda \rightarrow \Xi N$	0	0	$2P_+$	0
$\Lambda\Lambda \rightarrow \Sigma\Sigma$	0	$-\sqrt{3}P_+$	0	0
$\Xi N \rightarrow \Xi N$	0	-3	0	1
$\Xi N \rightarrow \Sigma\Sigma$	0	0	$2\sqrt{3}P_+$	0
$\Sigma\Sigma \rightarrow \Sigma\Sigma$	0	$-2P_+$	0	P_+
$\Xi N \rightarrow \Xi N$	1	1	0	1
$\Xi N \rightarrow \Sigma\Lambda$	1	0	$\sqrt{2}$	0
$\Xi N \rightarrow \Lambda\Sigma$	1	0	$-\sqrt{2}P_f$	0
$\Xi N \rightarrow \Sigma\Sigma$	1	0	$2\sqrt{2}P_-$	0
$\Sigma\Lambda \rightarrow \Sigma\Lambda$	1	0	0	1
$\Sigma\Lambda \rightarrow \Lambda\Sigma$	1	P_f	0	0
$\Sigma\Lambda \rightarrow \Sigma\Sigma$	1	$2P_-$	0	0
$\Sigma\Sigma \rightarrow \Sigma\Sigma$	1	$-P_-$	0	P_-
$\Sigma\Sigma \rightarrow \Sigma\Sigma$	2	P_+	0	P_+

SU(3) symmetry breaking in the meson-exchange contributions comes from the masses of the pseudoscalar mesons π , K , and η , for which we take the physical values [79].

The one-pseudoscalar-meson-exchange potential is given by

$$V_{B_1 B_2 \rightarrow B_3 B_4} = -f_{B_1 B_3 P} f_{B_2 B_4 P} \frac{(\boldsymbol{\sigma}_1 \cdot \mathbf{q})(\boldsymbol{\sigma}_2 \cdot \mathbf{q})}{\mathbf{q}^2 + m_P^2} \mathcal{I}_{B_1 B_2 \rightarrow B_3 B_4}, \quad (\text{A2})$$

where $f_{B_1 B_3 P}$, $f_{B_2 B_4 P}$ are the appropriate coupling constants as given in Eq. (A1) and m_P is the actual mass of the exchanged pseudoscalar meson. The transferred momentum, \mathbf{q} , is defined in terms of the initial (\mathbf{p}) and final (\mathbf{p}') center-of-mass (c.m.) momenta of the baryons as $\mathbf{q} = \mathbf{p}' - \mathbf{p}$. The isospin factors \mathcal{I} are summarized in Table IV. Explicit expressions for the momentum- and spin-dependent part of the two-meson exchange potentials can be found in Appendix A of Ref. [40]. Those expressions need to be multiplied with the appropriate combination of baryon-baryon-meson coupling constants and with the isospin factors. Since the list of isospin factors for two-pseudoscalar-meson exchanges is rather bulky for the $S = -2$ sector we collected the corresponding tables in a separate pdf file. The file can be obtained upon request directly from the authors. Note that the isospin factors for $\Sigma\Sigma$ with $I = 2$ have been published in Ref. [78].

For the ΞN and YY interactions there are couplings between channels with non-identical and with identical particles which requires special attention [93]. We follow the treatment of the flavor-exchange potentials as done by the Nijmegen group. Then the proper anti-symmetrization of the states is achieved by multiplying specific transitions with $\sqrt{2}$ factors that are included in Table IV, see Refs. [47]. In Table IV, P_f is the flavor-exchange operator having the values $P_f = 1$ for even-L (spin) singlet and odd-L triplet partial waves (antisymmetric in spin-momentum space), and $P_f = -1$ for odd-L singlet and even-L triplet partial waves (symmetric in spin-momentum space). For simplification of the notation we also introduce the operators $P_+ \equiv (1 + P_f)/2$ and $P_- \equiv (1 - P_f)/2$. Then $P_+ = 1$ ($P_- = 0$) for even-L singlet and odd-L triplet partial waves while $P_+ = 0$ ($P_- = 1$) for even-L triplet and odd-L single partial waves. We note that for $\Lambda\Lambda \rightarrow \Lambda\Lambda$, for example, η -exchange contributes only to spin-momentum space antisymmetric i.e. flavor symmetric partial waves, for example 1S_0 , $^3P_{0,1,2}$, etc.

For completeness all the LECs used in the present study are summarized in Tables V and VI. As said, most of the LECs are kept as given in Tables 3 and 4 of Ref. [40]. In this context let us mention, however, that unfortunately there are typos in Table 3 of that reference. The values for the LECs in the 10 and 10^* representations should be interchanged (for the 3S_1 partial wave and the 3S_1 - 3D_1 transition). Furthermore, the values for $\tilde{C}_{^3S_1}^{10^*}$ (labelled as $\tilde{C}_{^3S_1}^{10}$ in Ref. [40], cf. above) should read 0.104, 0.541, 1.49, 3.44, 4.99, and 5.60 for increasing cut-offs, i.e. the comma was misplaced in case of the last 4 entries.

TABLE V. Contact terms for the 1S_0 and 3S_1 - 3D_1 partial waves for various cut-offs. The values of the \tilde{C} 's are in 10^4 GeV^{-2} the ones of the C 's in 10^4 GeV^{-4} ; the values of Λ in MeV. (*) indicates the value of $\tilde{C}_{^3S_1}^{8a}$ from Ref. [40].

Λ		500	550	600	650
1S_0	$\tilde{C}_{^1S_0}^{27}$	0.1520	0.3296	0.6139	1.0752
	$\tilde{C}_{^1S_0}^{8s}$	0.1970	0.1930	0.1742	0.1670
	$\tilde{C}_{^1S_0}^1$	-0.015	-0.010	0.000	0.010
	$C_{^1S_0}^{27}$	2.260	2.260	2.260	2.260
	$C_{^1S_0}^{8s}$	-0.200	-0.206	-0.0816	-0.0597
	$C_{^1S_0}^1$	0.000	0.000	0.000	0.000
3S_1 - 3D_1	$\tilde{C}_{^3S_1}^{10*}$	0.541	1.49	3.44	4.99
	$\tilde{C}_{^3S_1}^{10}$	0.209	0.635	1.420	2.200
	$\tilde{C}_{^3S_1}^{8a}$	0.070	0.070	0.080	0.100
	$C_{^3S_1}^{10*}$	2.310	2.450	2.740	2.530
	$C_{^3S_1}^{10}$	0.143	0.741	1.090	1.150
	$C_{^3S_1}^{8a}$	0.469	0.627	0.775	0.854
	$C_{^3S_1-^3D_1}^{10*}$	-0.429	-0.428	-0.191	-0.191
	$C_{^3S_1-^3D_1}^{10}$	-0.300	-0.356	-0.380	-0.380
	$C_{^3S_1-^3D_1}^{8a}$	0.0475	0.0453	-0.00621	-0.00621
	$\tilde{C}_{^3S_1}^{8a}$ (*)	0.00715	-0.0143	-0.0276	-0.0269

TABLE VI. Contact terms for the P -waves for various cut-offs. The values of the LECs are in 10^4 GeV^{-4} ; the values of Λ in MeV.

Λ		500	550	600	650
3P_0	$C_{^3P_0}^{27}$	1.49	1.51	1.55	1.60
	$C_{^3P_0}^{8s}$	2.50	2.50	2.50	2.50
	$C_{^3P_0}^1$	-0.30	-0.30	-0.30	-0.30
3P_1	$C_{^3P_1}^{27}$	-0.43	-0.43	-0.43	-0.43
	$C_{^3P_1}^{8s}$	0.65	0.65	0.65	0.65
	$C_{^3P_1}^1$	-0.30	-0.30	-0.30	-0.30
3P_2	$C_{^3P_2}^{27}$	-0.063	-0.041	-0.025	-0.012
	$C_{^3P_2}^{8s}$	1.00	1.00	1.00	1.00
	$C_{^3P_2}^1$	-0.30	-0.30	-0.30	-0.30
1P_1	$C_{^1P_1}^{10}$	0.49	0.49	0.49	0.49
	$C_{^1P_1}^{10*}$	-0.14	-0.14	-0.14	-0.14
	$C_{^1P_1}^{8a}$	-0.35	-0.35	-0.35	-0.35
1P_1 - 3P_1	$C_{^1P_1-^3P_1}^{8s8a}$	0	0	0	0

-
- [1] R. L. Jaffe, Phys. Rev. Lett. **38**, 195 (1977) [Erratum-ibid. **38**, 617 (1977)].
[2] C. J. Yoon *et al.*, Phys. Rev. C **75**, 022201 (2007).
[3] B. H. Kim *et al.* [Belle Collaboration], Phys. Rev. Lett. **110**, 222002 (2013).
[4] S. R. Beane *et al.*, Phys. Rev. Lett. **106**, 162001 (2011).
[5] T. Inoue *et al.*, Phys. Rev. Lett. **106**, 162002 (2011).
[6] S. R. Beane *et al.*, Phys. Rev. D **85**, 054511 (2012).
[7] S. R. Beane *et al.*, Mod. Phys. Lett. A **26**, 2587 (2011).
[8] P. E. Shanahan, A. W. Thomas and R. D. Young, Phys. Rev. Lett. **107**, 092004 (2011).
[9] J. Haidenbauer and U.-G. Meißner, Phys. Lett. B **706**, 100 (2011).

- [10] J. Haidenbauer and U.-G. Meißner, Nucl. Phys. A **881**, 44 (2012).
- [11] T. Inoue *et al.*, Nucl. Phys. A **881** 28, (2012).
- [12] P. E. Shanahan, A. W. Thomas and R. D. Young, JPS Conf. Proc. **1**, 013028 (2014).
- [13] D. Chatterjee and I. Vidaña, arXiv:1510.06306 [nucl-th].
- [14] P. Demorest, T. Pennucci, S. Ransom, M. Roberts and J. Hessels, Nature **467**, 1081 (2010).
- [15] J. Antoniadis *et al.*, Science **340**, 1233232 (2013).
- [16] S. Weissenborn, D. Chatterjee and J. Schaffner-Bielich, Phys. Rev. C **85**, 065802 (2012) [Phys. Rev. C **90**, 019904 (2014)].
- [17] M. Oertel, C. Providencia, F. Gulminelli and A. R. Raduta, J. Phys. G **42**, 075202 (2015).
- [18] K. A. Maslov, E. E. Kolomeitsev and D. N. Voskresensky, Phys. Lett. B **748**, 369 (2015).
- [19] D. Lonardonì, F. Pederiva and S. Gandolfi, Phys. Rev. C **89**, 014314 (2014).
- [20] Y. Lim, C. H. Hyun, K. Kwak and C. H. Lee, arXiv:1412.5722 [nucl-th].
- [21] M. Yamaguchi, K. Tominaga, T. Ueda and Y. Yamamoto, Prog. Theor. Phys. **105**, 627 (2001).
- [22] E. Friedman and A. Gal, Phys. Rep. **452**, 89 (2007).
- [23] E. Hiyama, M. Kamimura, Y. Yamamoto, T. Motoba and T. A. Rijken, Prog. Theor. Phys. Suppl. **185**, 152 (2010).
- [24] P. Khaustov *et al.* [AGS E885 Collaboration], Phys. Rev. C **61**, 054603 (2000).
- [25] M. Kohno and S. Hashimoto, Prog. Theor. Phys. **123**, 157 (2010).
- [26] M. Kohno, Phys. Rev. C **81**, 014603 (2010).
- [27] K. Nakazawa *et al.*, Prog. Theor. Exp. Phys. **2015**, 033D02 (2015).
- [28] H. Garcilazo and A. Valcarce, Phys. Rev. C **92**, 014004 (2015).
- [29] H. Polinder, J. Haidenbauer and U.-G. Meißner, Phys. Lett. B **653**, 29 (2007).
- [30] S. Weinberg, Phys. Lett. B **251**, 288 (1990).
- [31] S. Weinberg, Nucl. Phys. B **363**, 3 (1991).
- [32] E. Epelbaum, W. Glöckle and U.-G. Meißner, Nucl. Phys. A **747**, 362 (2005).
- [33] E. Epelbaum, H. Krebs and U.-G. Meißner, Phys. Rev. Lett. **115**, 122301 (2015).
- [34] D. R. Entem and R. Machleidt, Phys. Rev. C **68** (2003) 041001.
- [35] D. R. Entem, N. Kaiser, R. Machleidt and Y. Nosyk, Phys. Rev. C **91**, 014002 (2015).
- [36] E. Epelbaum, Prog. Part. Nucl. Phys. **57**, 654 (2006).
- [37] R. Machleidt and D. R. Entem, Phys. Rep. **503**, 1 (2011).
- [38] C. L. Korpa, A. E. L. Dieperink and R. G. E. Timmermans, Phys. Rev. C **65**, 015208 (2001).
- [39] H. Polinder, J. Haidenbauer and U.-G. Meißner, Nucl. Phys. A **779**, 244 (2006).
- [40] J. Haidenbauer, S. Petschauer, N. Kaiser, U.-G. Meißner, A. Nogga and W. Weise, Nucl. Phys. A **915**, 24 (2013).
- [41] J. Haidenbauer and U. G. Meißner, Nucl. Phys. A **936**, 29 (2015).
- [42] S. Petschauer, J. Haidenbauer, N. Kaiser, U. G. Meißner and W. Weise, arXiv:1507.08808 [nucl-th]; Eur. Phys. J. A, in print.
- [43] J. K. Ahn *et al.* [E224 Collaboration], Nucl. Phys. A **625**, 231 (1997).
- [44] J. K. Ahn *et al.*, Phys. Lett. B **633**, 214 (2006).
- [45] S. Aoki *et al.*, Nucl. Phys. A **644**, 365 (1998).
- [46] K. Tominaga, T. Ueda, M. Yamaguchi, N. Kijima, D. Okamoto, K. Miyagawa and T. Yamada, Nucl. Phys. A **642**, 483 (1998).
- [47] V.G.J. Stoks and Th.A. Rijken, Phys. Rev. C **59**, 3009 (1999).
- [48] T. A. Rijken and Y. Yamamoto, Phys. Rev. C **73**, 044008 (2006).
- [49] Y. Fujiwara, Y. Suzuki and C. Nakamoto, Prog. Part. Nucl. Phys. **58**, 439 (2007).
- [50] T. A. Rijken, M. M. Nagels and Y. Yamamoto, Prog. Theor. Phys. Suppl. **185**, 14 (2010).
- [51] S. Petschauer, N. Kaiser, J. Haidenbauer, U.-G. Meißner and W. Weise, arXiv:1511.02095.
- [52] A. M. Gasparyan, J. Haidenbauer and C. Hanhart, Phys. Rev. C **85**, 015204 (2012).
- [53] H. Takahashi *et al.*, Phys. Rev. Lett. **87**, 212502 (2001).
- [54] K. Nakazawa, Nucl. Phys. A **835**, 207 (2010).
- [55] I. N. Filikhin and A. Gal, Nucl. Phys. A **707**, 491 (2002).
- [56] I.R. Afnan and B.F. Gibson, Phys. Rev. C **67**, 017001 (2003).
- [57] I. Filikhin, A. Gal and V. M. Suslov, Nucl. Phys. A **743**, 194 (2004).
- [58] T. Yamada, Phys. Rev. C **69**, 044301 (2004).
- [59] I. Vidaña, A. Ramos and A. Polls, Phys. Rev. C **70**, 024306 (2004).
- [60] Q. N. Usmani, A. R. Bodmer and B. Sharma, Phys. Rev. C **70**, 061001 (2004).
- [61] H. Nemura, S. Shinmura, Y. Akaishi and K.S. Myint, Phys. Rev. Lett. **94**, 202502 (2005).
- [62] A. Gasparyan, J. Haidenbauer, C. Hanhart and J. Speth, Phys. Rev. C **69**, 034006 (2004).
- [63] K. Morita, T. Furumoto and A. Ohnishi, Phys. Rev. C **91**, 024916 (2015).
- [64] L. Adamczyk *et al.* [STAR Collaboration], Phys. Rev. Lett. **114**, 022301 (2015).
- [65] S. J. Kim, presentation at the *12th International Conference on Hypernuclear and Strange Particle Physics*, Sendai, Japan, 2015, see <http://lambda.phys.tohoku.ac.jp/hyp2015/>
- [66] T. Tamagawa *et al.*, Nucl. Phys. A **691**, 234c (2001).
- [67] G. R. Charlton *et al.*, Phys. Lett. **32B**, 720 (1970).
- [68] R. A. Muller Phys. Lett. **38B**, 123 (1972).
- [69] R.R.A. Dalmeijer, A. J. De Groot, J.C. Kluyver, E. De Lijser and H.J.G.M. Tiecke, Lett. Nuovo Cim. **4**, 373 (1970).
- [70] J.M. Hauptman, J.A. Kadyk and G.H. Trilling, Nucl. Phys. B **125**, 29 (1977).

- [71] D.P. Goyal, J.N. Misra and A.V. Sodhi, Phys. Rev. D **21**, 607 (1980).
- [72] G. d'Agostini et al., Nucl. Phys. B **209**, 1 (1982).
- [73] M. Godbersen, AIP Conf. Proc. **338**, 533 (1995).
- [74] M. Kohno, Y. Fujiwara and Y. Suzuki, Nucl. Phys. A **835**, 358 (2010).
- [75] S. Petschauer and N. Kaiser, Nucl. Phys. A **916**, 1 (2013).
- [76] J. J. de Swart, Rev. Mod. Phys. **35**, 916 (1963).
- [77] C. B. Dover and H. Feshbach, Annals Phys. **198**, 321 (1990).
- [78] J. Haidenbauer, U.-G. Meißner and S. Petschauer, Eur. Phys. J. A **51**, 17 (2015).
- [79] K.A. Olive *et al.* (Particle Data Group), Chin. Phys. C **38**, 090001 (2014).
- [80] R.A. Arndt, W.J. Briscoe, I.I. Strakovsky and R.L. Workman, Phys. Rev. C **76**, 025209 (2007);
<http://gwdac.phys.gwu.edu/>
- [81] G. Q. Li and R. Machleidt, Phys. Rev. C **48**, 1702 (1993).
- [82] H.-J. Schulze, A. Schnell, G. Ropke and U. Lombardo, Phys. Rev. C **55**, 3006 (1997).
- [83] M. Kohno, M. Higashi, Y. Watanabe and M. Kawai, Phys. Rev. C **57**, 3495 (1998).
- [84] R. J. Furnstahl, D. R. Phillips, and S. Wesolowski, J. Phys. G **42**, 034028 (2015).
- [85] E. Epelbaum, H. Krebs, and U.-G. Meißner, Eur. Phys. J. A **51**, 53 (2015).
- [86] R. J. Furnstahl, N. Klco, D. R. Phillips, and S. Wesolowski, Phys. Rev. C **92**, 024005 (2015).
- [87] A. M. Badalian, L. P. Kok, M. I. Polikarpov, Y. A. Simonov, Phys. Rep. **82**, 31 (1982).
- [88] K. Sasaki, S. Aoki, T. Doi, T. Hatsuda, Y. Ikeda, T. Inoue, N. Ishii and K. Murano, arXiv:1504.01717 [hep-lat].
- [89] K. Sasaki, presentation at the *12th International Conference on Hypernuclear and Strange Particle Physics*, Sendai, Japan, 2015, see <http://lambda.phys.tohoku.ac.jp/hyp2015/>
- [90] K. Aoki et al., Proposal P05, J-PARC PAC-01, 2006,
http://j-parc.jp/researcher/Hadron/en/pac_0606/pdf/p05-Nagae.pdf
- [91] U. Wiedner, Prog. Part. Nucl. Phys. **66**, 477 (2011).
- [92] A. Sanchez Lorente [Panda Collaboration], Hyperfine Interact. **229**, 45 (2014).
- [93] K. Miyagawa, H. Kamada and W. Glöckle, Nucl. Phys. A **614**, 535 (1997).